Diversity of Metal-Organic Macrocycles Assembled from Carbazole Based Ligands with Different Length

Hao Yu, Jing Wang, Xiangyang Guo, Rong Zhang*, Cheng He* and Chunying Duan

1. Syntheses and Characterizations

1.1 Materials and measurements

All chemicals were of reagent grade quality obtained from commercial sources and used without further purification. CH_3CN was distilled from calcium hydride for use. ^1H-NMR and ^{13}C-NMR spectra were measured on a Varian INOVA 400 M and 500 M spectrometer. ESI-MS and IM-MS spectra were carried out on a HPLC-Q-Tof MS, Accurate TOF LC/MS and Ion Mobility spectrometer. The elemental analyses of C, H and N were performed on a Vario EL III elemental analyzer.

1.2 Synthesis

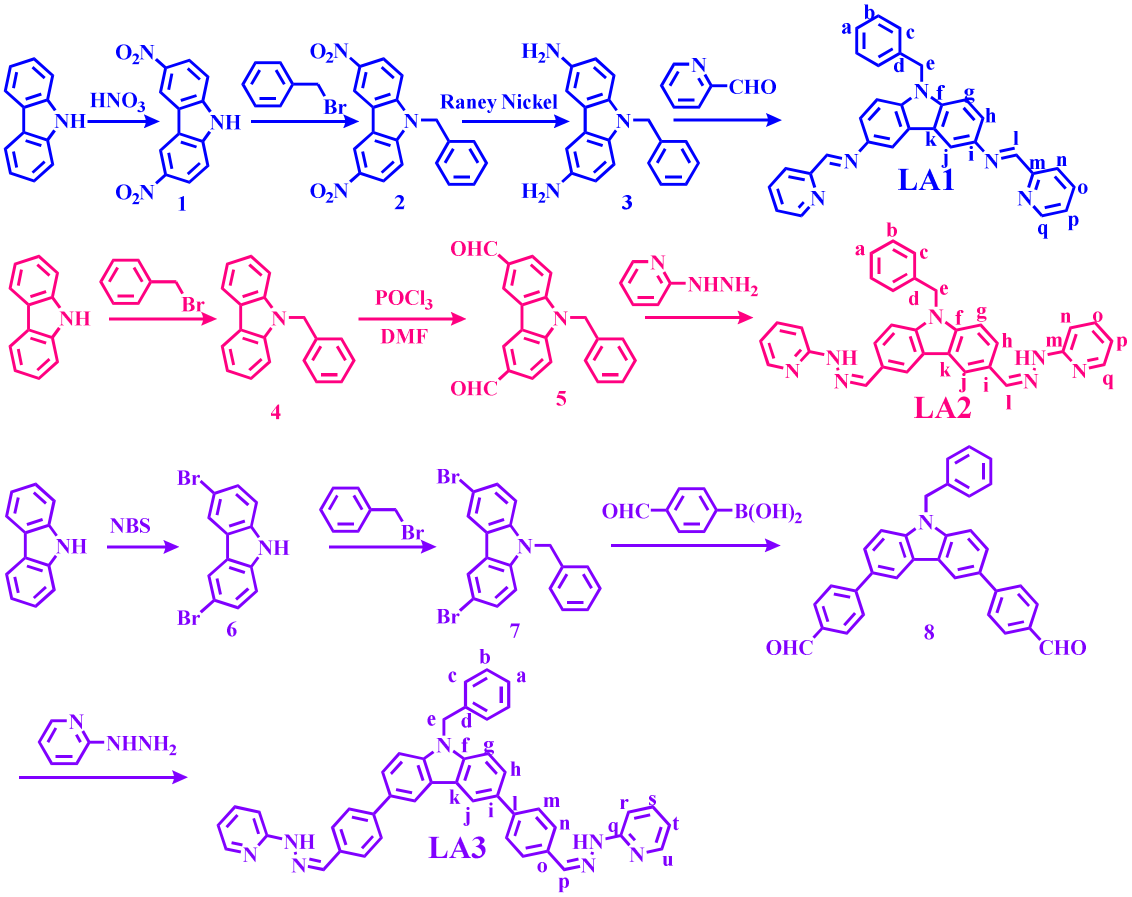

Fig. S1 Synthesis of ligand **LA1**, **LA2** and **LA3**.

3,6-dinitro-9H-carbazole (1)[1]. A three-necked round-bottomed flask, equipped with condenser, addition funnel, and stirring bar, was charged with carbazole (10.03 g, 60.0 mmol) and glacial AcOH (80 g) under Ar. The mixture was stirred for 1.5 h at 40 °C. Then, 10% HNO_3/AcOH (1:1, 16.4 g) was added dropwise and the mixture was stirred for 2 h at 90-100 °C. The yellow precipitate was filtered and washed with cold AcOH (50 mL) and then with water. The solid was warmed in KOH/EtOH (200 mL, 60 g/L) at 50 °C for 30 min and filtered. The insoluble red solid was digested in 10% HCl at 100 °C for 2 h. The resulting yellow solid was filtered, washed with water, and dried overnight under vacuum. ^{1}H NMR (DMSO-*d6*, 400 M) δ 12.73 (s, $1H_{NH}$), 9.47 (d, $2H_{carbazole}$), 8.36 (dd, $2H_{carbazole}$ J_1 = 9.3, J_2 = 2.7 Hz), 7.74 (d, $2H_{carbazole}$, J = 9.0 Hz).

9-benzyl-3,6-dinitro-9H-carbazole (2). A solution of **1** (10.4 g, 30 mmol) and KOH (3.4 g, 60 mmol) in dimethyl sulfoxide (100 mL) under stirring was heated at 90 °C for 4 h, and then benzyl bromide (5.1 g, 30 mmol) was gradually added. After being stirred for another 48 h at 90 °C, the mixture was poured into water (100 mL) and filtered. The residue was washed with water (200 mL × 3) and then dried overnight under vacuum. The yellow precipitate was recrystallized from ethanol to give the pure product. Yield: 7.6 g, 73%. ^{1}H NMR (DMSO-*d6*, 400 MHz, ppm): δ 5.5 (s, $2H_{CH2}$), 7.1 - 7.3 (m, $5H_{C6H5}$), 7.96 (d, $2H_{carbazole}$, J = 9.0 Hz), 8.44 (dd, $2H_{carbazole}$ J_1 = 9.3 Hz, J_2 = 2.7 Hz), 9.52 (d, $2H_{carbazole}$).

9-benzyl-3,6-diamine-9H-carbazole (3). **2** (3.47 g, 10 mmol) and Raney nickel (4.0 g, excess) were added to 100 mL of CH_2Cl_2, then hydrazine hydrate (2.0 g) was added and the mixture was filtered after reacting at room temperature for 3 h. The solvent was removed by vacuum rotary evaporation to give a grey product 1.89 g in a yield of about 66%. ^{1}H NMR (DMSO-*d6*, 400 MHz, ppm): δ 4.58(s, $4H_{NH2}$), 5.69 (s, $2H_{CH2}$), 6.7 - 7.3 (m, $11H_{C6H5\ carbazole}$).

Ligand LA1. 2-pyridinecarboxaldehyde (1.28 g, 12 mmol) was added to a methanol solution (50 mL) containing **3** (1.44 g, 5 mmol). After 5 drops of acetic acid was added, the mixture was refluxed for 12 h. The yellow solid was collected by filtration, washed with methanol and dried under vacuum. Yield: 1.35 g, 58%. ^{1}H NMR (DMSO-*d6*, 500 MHz, ppm): δ 5.73 (s, $2H_{CH2}$), 7.1 - 7.3 (m, $5H_{C6H5}$), 7.6 - 8.8 (m, $14H_{pyridine\ carbazole}$), 8.84 (s, $2H_{N=CH}$). ^{13}C NMR (DMSO-*d6*, 500 MHz, ppm): δ 157.95 (l), 154.57 (q), 149.64 (m), 142.46 (i), 140.13 (n), 137.59 (d), 136.97 (o), 128.63 (f), 127,34 (b), 126.74 (c), 125.16 (p), 123.16 (a), 121.10 (j), 120.78 (k), 113.51 (g), 110.37 (h), 45.91 (e). Anal. Calc. for ($C_{31}H_{23}N_5$): H, 4.98; C, 79.98; N, 15.04; Found: H, 5.10; C, 78.46; N, 14.76. ESI-MS *m/z*: 466.5 $[M+H]^+$.

Ni-**LA1**. A solution of $Ni(ClO_4)_2{\cdot}6H_2O$ (73.1 mg, 0.2 mmol) and ligand **LA1** (46.5 mg, 0.1 mmol) in 40 mL CH_3CN/CH_3OH (v/v, 9:1) was stirred at room temperature for 12 h, red needle-like crystals of Ni-**LA1** were obtained by diffusing diethyl ether into the aforementioned CH_3CN/CH_3OH solution. Yield: about 50%. Anal. Calc. for $Ni_2(C_{31}H_{23}N_5)_2(CH_3CN)_4(ClO_4)_4$: H, 3.63; C, 52.21; N, 12.18; Found: H, 3.70; C, 52.32; N, 12.30.

ESI mass spectra *m/z*: 262.07 $[Ni_2(\mathbf{LA1})_2]^{4+}$, 382.40 $[Ni_2(\mathbf{LA1})_2(ClO_4^-)]^{3+}$, 623.08 $[Ni_2(\mathbf{LA1})_2(ClO_4^-)_2]^{2+}$ and 1345.11 $[Ni_2(\mathbf{LA1})_2(ClO_4^-)_3]^+$, respectively.

The simulation based on natural isotopic abundance *m/z*: 262.06 $[Ni_2(\mathbf{LA1})_2]^{4+}$, 382.41 $[Ni_2(\mathbf{LA1})_2(ClO_4^-)]^{3+}$, 623.08 $[Ni_2(\mathbf{LA1})_2(ClO_4^-)_2]^{2+}$ and 1345.12 $[Ni_2(\mathbf{LA1})_2(ClO_4^-)_3]^{+}$, respectively.

9-benzyl-9H-carbazole (4)[2]: A solution of carbazole (5.0 g, 30 mmol) and KOH (3.4 g, 60 mmol) in dimethyl sulfoxide (100 mL) under stirring was heated at 90 °C for 4 h, and then benzyl bromide (5.1 g, 30 mmol) was gradually added. After being stirred for another 48 h at 90 °C, the mixture was poured into water (100 mL) and extracted with dichloromethane. The organic layer was washed with water (100 mL × 3) and brine (100 mL × 3), and then dried over anhydrous magnesium sulfate. The solvent was removed by vacuum rotary evaporation to obtain a crude product. The residue was purified by silica gel column chromatography (dichloromethane/petroleum ether, 1:1 as an eluent). Yield: 6.8 g, 88%. ^1H NMR (DMSO-*d6*, 400 MHz, ppm): δ 5.5 (s, $2H_{CH2}$), 7.1 - 8.1 (m, $13H_{C6H5\ carbazole}$).

9-benzyl-9H-carbazole-3,6-dicarbaldehyde (5). Phosphoryl chloride (21.5 g, 140 mmol) was added dropwise to a solution of N,N-dimethylformamide (12.4 g, 170 mmol) in 1,2-dichloroethane (10 mL) at 0 °C. Then the reaction mixture was heated to 35 °C, and a solution of **4** (2.6 g, 10 mmol) in 1,2-dichloroethane (40 mL) was added. After being stirred for 48 h at 90 °C, the mixture was poured into water (200 mL) and extracted with dichloromethane. The organic layer was washed with water (100 mL × 3) and brine (100 mL × 3), and then dried over anhydrous magnesium sulfate. The solvent was removed by vacuum rotary evaporation. The residue was purified by silica gel column chromatography (dichloromethane/petroleum ether, 4:1 as an eluent). Yield: 1.7 g, 53%. ^1H NMR ($CDCl_3$, 400 MHz, ppm): δ 5.6 (s, $2H_{CH2}$), 7.1 - 8.9 (m, $11H_{C6H5\ carbazole}$), 10.1 (s, $2H_{CH=O}$).

Ligand LA2. 2-hydrazinylpyridine (1.31 g, 12 mmol) was added to a methanol solution (50 mL) containing **2** (1.56 g, 5 mmol). After 5 drops of acetic acid was added, the mixture was refluxed for 12 h. The yellow solid was collected by filtration, washed with methanol and dried under vacuum. Yield: 1.91 g, 77%. ^1H NMR (DMSO-*d6*, 500 MHz, ppm): δ 10.79 (s, $2H_{NNH}$), 8.51 (s, $2H_{carbazole}$), 8.46 (s, $2H_{N=CH}$), 6.5 - 8.0 (m, $17H_{C6H5\ carbazole\ pyridine}$), 5.71 (s, $2H_{CH2}$). ^{13}C NMR (DMSO-*d6*, 500 MHz, ppm): δ 157.30 (m), 147.72 (q), 140.80 (l), 139.93 (k), 137.80 (o), 137.47 (d), 128.61 (f), 128.55 (b), 127.32 (c), 126.71 (g), 124.03 (a), 122.54 (i), 119.10 (j), 114.47 (p), 110.22 (h), 106.29 (n), 45.80 (e). Anal. Calc. for ($C_{31}H_{25}N_7$): H, 5.08; C, 75.13; N, 19.78; Found: H, 5.20; C, 74.53; N, 19.47. ESI-MS *m/z*: 496.4 $[M+H]^+$.

Ni-**LA2**. A solution of $Ni(ClO_4)_2{\cdot}6H_2O$ (73.1 mg, 0.2 mmol) and ligand **LA2** (49.5 mg, 0.1 mmol) in 40 mL CH_3CN/CH_3OH (v/v, 9:1) was stirred at room temperature for 12 h, a large amount of yellow needle-like crystals of Ni-**LA2[44]** and few yellow square-shaped crystals Ni-**LA2[22]** were obtained by diffusing diethyl ether into the aforementioned CH_3CN/CH_3OH solution.

ESI mass spectra *m/z*: 402.42 [Ni_2(**LA2**)$_2$(ClO_4^-)]$^{3+}$, 503.09 [Ni_4(**LA2**)$_4$(ClO_4^-)$_3$]$^{5+}$, 653.10 [Ni_2(**LA2**)$_2$(ClO_4^-)$_2$]$^{2+}$/[Ni_4(**LA2**)$_4$(ClO_4^-)$_4$]$^{4+}$, 904.45 [Ni_4(**LA2**)$_4$(ClO_4^-)$_5$]$^{3+}$ and 1406.15 [Ni_4(**LA2**)$_4$(ClO_4^-)$_6$]$^{2+}$/[Ni_2(**LA2**)$_2$(ClO_4^-)$_3$]$^{+}$, respectively.

The simulation based on natural isotopic abundance *m/z*: 402.42 [Ni_2(**LA2**)$_2$(ClO_4^-)]$^{3+}$, 503.10 [Ni_4(**LA2**)$_4$(ClO_4^-)$_3$]$^{5+}$, 653.11 [Ni_2(**LA2**)$_2$(ClO_4^-)$_2$]$^{2+}$, 653.61 [Ni_4(**LA2**)$_4$(ClO_4^-)$_4$]$^{4+}$, 904.46 [Ni_4(**LA2**)$_4$(ClO_4^-)$_5$]$^{3+}$, 1405.16 [Ni_2(**LA2**)$_2$(ClO_4^-)$_3$]$^{+}$ and 1406.17 [Ni_4(**LA2**)$_4$(ClO_4^-)$_6$]$^{2+}$, respectively.

3,6-dibromo-9H-carbazole (6)[3]. A solution of NBS (42.72 g, 240 mmol) in 200 mL DMF was added slowly to a suspension of carbazole (20 g, 120 mmol) in dichloromethane (1.2 L). The reaction mixture was stirred at room temperature and the progress of the reaction was controlled by GCMS analysis. Then the solution was washed with water (200 mL × 3), the organic layer was dried under magnesium sulfate and filtered. The solvent was evaporated and the residue was dissolved in acetone (100 mL) and precipitated with hexane (600 mL). 3,6-dibromo-9H-carbazole was filtered and dried under vacuum to afford a grey product. Yield: 35 g, 90%. ^{1}H NMR ($CDCl_3$, 400 MHz, ppm): δ 7.31 (d, 2H, J = 6.8 Hz), 7.52 (d, 2H, J_1 = 6.9, J_2 = 1.5), 8.13 (d, 2H, J = 1.3 Hz), 10.37 (s, 1H_{NH}).

9-benzyl-3,6-dibromo-9H-carbazole (7). A solution of **6** (9.75 g, 30 mmol) and KOH (3.4 g, 60 mmol) in dimethyl sulfoxide (100 mL) under stirring was heated at 90 °C for 4 h, and then benzyl bromide (5.1 g, 30 mmol) was gradually added. After being stirred for another 48 h at 90 °C, the mixture was poured into water (100 mL) and extracted with dichloromethane. The organic layer was washed with water (100 mL × 3) and brine (100 mL × 3), and then dried over anhydrous magnesium sulfate. The solvent was removed by vacuum rotary evaporation to obtain a crude product. The residue was purified by silica gel column chromatography (dichloromethane/petroleum ether, 1:1 as an eluent). Yield: 8.7 g, 70%. ^{1}H NMR (DMSO-*d6*, 400 MHz, ppm): δ 5.69 (s, 2H_{CH2}), 7.1 -7.3 (m, 5H_{C6H5}), 7.5 - 8.5 (m, 6$H_{carbazole}$).

4,4'-(9-benzyl-9H-carbazole-3,6-diyl)dibenzaldehyde (8). Under a nitrogen atmosphere, to a solution of **7** (4.15 g, 10 mmol) in 1,4-dioxane/H_2O solvent (1:1, 200 mL) were added (4-formylphenyl)boronic acid (3.3 g, 22 mmol), $Pd(PPh_3)_4$ (0.093 g, 0.05 mmol) and K_2CO_3 (13.8 g, 100 mmol). After the mixture was stirred at 100 °C for 48 h, then filtered and concentrated. The crude product was purified by column chromatography on silica gel with dichloromethane to give pure **8** as a gray solid. Yield: 3.8 g, 82%. ^{1}H NMR (DMSO-*d6*, 500 MHz, ppm): δ 5.78 (s, 2H_{CH2}), 7.2 - 7.3 (m, 5H_{C6H5}), 7.8 - 8.9 (m, 14$H_{C6H4\ carbazole}$), 10.07 (s, 2H_{CHO}).

Ligand LA3. 2-hydrazinylpyridine (1.31 g, 12 mmol) was added to a methanol solution (50 mL) containing **8** (2.33 g, 5 mmol). After 5 drops of acetic acid was added, the mixture was refluxed for 12 h. The yellow solid was collected by filtration, washed with methanol and dried under vacuum. Yield: 1.7 g, 53%. ^{1}H NMR (DMSO-*d6*, 500 MHz, ppm): δ 5.74 (s, 2H_{CH2}), 6.7 -8.2 (m, 27H_{C6H5}

$_{\mathrm{C6H4\ carbazole\ pyridine}}$), 8.74 (s, $2H_{N=CH}$), 10.91 (s, $2H_{NNH}$). ^{13}C NMR (DMSO-*d6*, 500 MHz, ppm): δ 157.06 (q), 147.77 (u), 140.87 (i), 140.33 (p), 138.61 (l), 137.89 (s), 137.66 (d), 133.62 (f), 130.99(o), 128.61 (n), 127.30 (b), 126.82 (m), 126.72 (c), 126.50 (a), 124.93 (j), 123.20 (t), 118.76 (k), 114.89 (g), 110.19 (h), 106.32 (r), 45.80 (e). Anal. Calc. for ($C_{43}H_{33}N_7$): H, 5.14; C, 79.73; N, 15.14; Found: H, 5.27; C, 78.67; N, 14.85. ESI-MS *m/z*: 648.7 $[M+H]^+$.

Ni-**LA3**. A solution of $Ni(ClO_4)_2 \cdot 6H_2O$ (73.1 mg, 0.2 mmol) and ligand **LA3** (64.8 mg, 0.1 mmol) in 40 mL CH_3CN/CH_3OH (v/v, 9:1) was stirred at room temperature for 12 h.

ESI mass spectra *m/z*: 352.99 $[\mathrm{Ni}_2(\mathbf{LA3})_2]^{4+}$, 443.57 $[\mathrm{Ni}_3(\mathbf{LA3})_3(\mathrm{ClO}_4^-)]^{5+}$, 503.63 $[\mathrm{Ni}_2(\mathbf{LA3})_2(\mathrm{ClO}_4^-)]^{3+}$, 579.19 $[\mathrm{Ni}_3(\mathbf{LA3})_3(\mathrm{ClO}_4^-)_2]^{4+}$, 624.33 $[\mathrm{Ni}_4(\mathbf{LA3})_4(\mathrm{ClO}_4^-)_3]^{5+}$, 804.90 $[\mathrm{Ni}_2(\mathbf{LA3})_2(\mathrm{ClO}_4^-)_2]^{2+}$/ $[\mathrm{Ni}_3(\mathbf{LA3})_3(\mathrm{ClO}_4^-)_3]^{3+}$, 1031.86 $[\mathrm{Ni}_5(\mathbf{LA3})_5(\mathrm{ClO}_4^-)_6]^{4+}$, 1107.18 $[\mathrm{Ni}_4(\mathbf{LA3})_4(\mathrm{ClO}_4^-)_5]^{3+}$, 1257.81 $[\mathrm{Ni}_3(\mathbf{LA3})_3(\mathrm{ClO}_4^-)_4]^{2+}$/$[\mathrm{Ni}_6(\mathbf{LA3})_6(\mathrm{ClO}_4^-)_8]^{4+}$ and 1408.76 $[\mathrm{Ni}_5(\mathbf{LA3})_5(\mathrm{ClO}_4^-)_7]^{3+}$, respectively.

The simulation based on natural isotopic abundance *m/z*: 353.11 $[\mathrm{Ni}_2(\mathbf{LA3})_2]^{4+}$, 443.72 $[\mathrm{Ni}_3(\mathbf{LA3})_3(\mathrm{ClO}_4^-)]^{5+}$, 503.79 $[\mathrm{Ni}_2(\mathbf{LA3})_2(\mathrm{ClO}_4^-)]^{3+}$, 579.39 $[\mathrm{Ni}_3(\mathbf{LA3})_3(\mathrm{ClO}_4^-)_2]^{4+}$, 624.75 $[\mathrm{Ni}_4(\mathbf{LA3})_4(\mathrm{ClO}_4^-)_3]^{5+}$, 805.17 $[\mathrm{Ni}_2(\mathbf{LA3})_2(\mathrm{ClO}_4^-)_2]^{2+}$, 805.50 $[\mathrm{Ni}_3(\mathbf{LA3})_3(\mathrm{ClO}_4^-)_3]^{3+}$, 1031.95 $[\mathrm{Ni}_5(\mathbf{LA3})_5(\mathrm{ClO}_4^-)_6]^{4+}$, 1107.55 $[\mathrm{Ni}_4(\mathbf{LA3})_4(\mathrm{ClO}_4^-)_5]^{3+}$, 1257.73 $[\mathrm{Ni}_3(\mathbf{LA3})_3(\mathrm{ClO}_4^-)_4]^{2+}$, 1258.48 $[\mathrm{Ni}_6(\mathbf{LA3})_6(\mathrm{ClO}_4^-)_8]^{4+}$ and 1409.26 $[\mathrm{Ni}_5(\mathbf{LA3})_5(\mathrm{ClO}_4^-)_7]^{3+}$, respectively.

2. Crystallography

The intensities were collected on a Bruker SMART APEX CCD diffractometer equipped with a graphite-monochromated Mo−Kα (λ = 0.71073 Å) radiation source; the data were acquired using the SMART and SAINT programs [4]. The structures were solved by direct methods and refined on F2 by full-matrix least-squares methods using the SHELXTL version 5.1 software [5].

Crystal data for Ni-**LA1**. $Ni_2C_{70}H_{58}Cl_4N_{14}O_{16}$, Mr= 1610.52, Orthorhombic, space group Pbcn, red needle-like crystal, a = 16.416(3) Å, b = 31.885(5) Å, c = 15.264(3) Å, V = 7989(2) Å^3, Z = 4, μ (MoKα) = 0.675 mm^{-1}, T = 200(2) K, 7012 unique reflections [R_{int} = 0.1265], Final R_1 [with $I > 2\sigma(I)$] = 0.0837, wR_2 (all data) = 0.1845. **CCDC NO. 1815437**

Crystal data for Ni-**LA2[22]**. $Ni_4C_{145}H_{138}Cl_8N_{37}O_{34.50}$, Mr= 3469.36, Monoclinic, space group $P2_1/c$, yellow square-shaped crystal, a = 34.426(1) Å, b = 13.971(1) Å, c = 33.542(1) Å, , β = 96.03(1)°, V = 16043.1(5) Å^3, Z = 4, μ(MoKα) = 0.681 mm^{-1}, T = 200(2) K, 28131 unique reflections [R_{int} = 0.0564], Final R_1 [with $I > 2\sigma(I)$] = 0.0769, wR_2 (all data) = 0.2319. **CCDC NO. 1815438**.

Crystal data for Ni-**LA2[44]**. $Ni_4C_{150}H_{155}Cl_8N_{37}O_{38}$, Mr= 3602.55, Triclinic, space group P-1, yellow needle-like crystal, a = 12.135(1) Å, b = 17.558(1) Å, c = 22.164(2) Å, α = 98.47(1)°, β = 100.41(1)°, γ = 109.07(1)°, V = 4280.5(6) Å^3, Z = 1, μ (MoKα) = 0.642 mm^{-1}, T = 150(2) K, 14988 unique reflections [R_{int} = 0.1564], Final R_1 [with $I > 2\sigma(I)$] = 0.0898, wR_2 (all data) = 0.2011. **CCDC NO. 1815440**.

In the structural refinement of Ni-**LA1**, the benzene ring in the carbazole moiety, four carbon atoms in one pyridine ring and one terminal carbon atom in the coordinated acetonitrile molecule were disordered into two parts with each site occupy factor (s. o. f.) being fixed at 0.5. Several oxygen atoms in the perchlorate ions were also disordered into two parts with each s. o. f. being fixed equally. Except the disordered parts in the structure, non-hydrogen atoms were refined anisotropically. Hydrogen atoms within the ligand backbones and the solvent molecules were fixed geometrically at calculated distances and allowed to ride on the parent non-hydrogen atoms. To assist the stability of refinements, the disordered pyridine ring was restrained as idealized regular polygons. For the A and B alert in checkcif, the ratio observed /unique reflections were too low because that the weak diffraction intensity of the crystal. The short distance between intermolecular O atoms is due to the partly occupied perchlorate ion being symmetrically disordered. The disordered atom in main skeleton were not refined anisotropically.

In the structural refinement of Ni-**LA2[22]**, one coordinated ligand on the Ni center was assigned as half water molecule and half coordinated acetonitrile molecule with the oxygen atom and the nitrogen atom share the same site. Four carbon atoms in one benzene ring in the carbazole moiety, three terminal carbon atoms in respective coordinated acetonitrile molecules, several oxygen atoms and one chloride atoms in the perchlorate ions were disordered into two parts with each s. o. f. being fixed with suitable value. Except the disordered parts and partly occupied solvent molecules in the structure, non-hydrogen atoms were refined anisotropically. Except the half-occupied coordination water molecule, hydrogen atoms within the ligand backbones and the solvent molecules were fixed geometrically at calculated distances and allowed to ride on the parent non-hydrogen atoms. The disordered benzene ring and the solvent dimethyl ether molecule were restrained as idealized regular polygons. For the A and B alert in checkcif, the short intra H… H distance is due to the strong stacking interaction and the fixed coordination configuration, thus the ligands could only be rotated in a certain range resulting in some H atoms have to be close to each other. And some disordered atoms in main skeleton were not refined anisotropically. No hydrogen bond interaction could be found for the solvent water molecules, possibly due to the presence of highly disordered free solvent molecules which could not be found in the electronic density map.

In the structural refinement of Ni-**LA2[44]**, one coordinated ligand on the Ni center was assigned as half water molecule and half coordinated acetonitrile molecule with the oxygen atom and the nitrogen atom share the same site. Two terminal carbon atoms in respective coordinated acetonitrile molecules, several oxygen atoms and one chloride atoms in the perchlorate ions were disordered into two parts with each s. o. f. being fixed with suitable value. One disordered perchlorate ion was restrained as idealized regular polygons, thermal parameters on adjacent atoms in them were restrained to be similar. The distances in several solvent dimethyl ether and acetonitrile molecules were restrained as idealized value. For the B alert in checkcif, the ratio observed /unique reflections were too low because that the weak diffraction intensity of the crystal. No hydrogen bond interaction could be found for the coordinated and solvent water molecules, possibly due to the presence of highly disordered free solvent molecules which could not be found in the electronic density map.

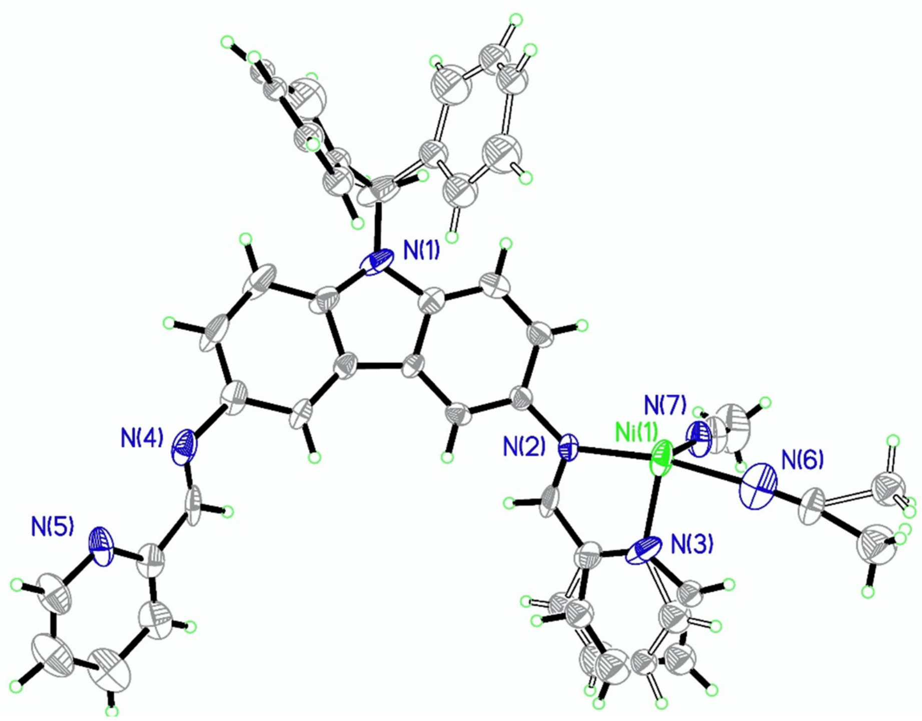

Fig. S2 Molecular structure of Ni-**LA1** within an unique asymmetric unit, showing the backbone of the ligand in the complex. Selected bond distances (Å) and angles (°): Ni(1)-N(6) 2.017(9), Ni(1)-N(7) 2.049(7), Ni(1)-N(5)#1 2.062(8), Ni(1)-N(3) 2.070(8), Ni(1)-N(4)#1 2.096(7), Ni(1)-N(2) 2.103(6), N(1)-C(14) 1.367(9), N(1)-C(8) 1.387(9), N(1)-C(7) 1.480(9), N(2)-C(20) 1.312(9), N(2)-C(11) 1.436(9), N(3)-C(25) 1.306(19), N(3)-C(21) 1.331(12), N(3)-C(25') 1.53(3), N(4)-C(26) 1.283(10), N(4)-C(17) 1.440(10), N(4)-Ni(1)#1 2.096(7), N(5)-C(31) 1.309(9), N(5)-C(27) 1.369(10), N(5)-Ni(1)#1 2.062(8), N(6)-C(32) 1.129(13), N(7)-C(34) 1.118(9), C(1)-C(2) 1.422(15), C(1)-C(6) 1.430(13), C(1)-C(7) 1.430(14), C(2)-C(3) 1.395(15), C(3)-C(4) 1.246(12), C(4)-C(5) 1.272(13), C(5)-C(6) 1.490(14), C(1')-C(6') 1.395(14), C(1')-C(2') 1.455(14), C(1')-C(7) 1.880(16), C(2')-C(3') 1.346(14), C(3')-C(4') 1.238(13), C(4')-C(5') 1.433(14), C(5')-C(6') 1.372(15), C(8)-C(9) 1.398(10), C(8)-C(13) 1.418(9), C(9)-C(10) 1.414(10), C(10)-C(11) 1.405(9), C(11)-C(12) 1.389(9), C(12)-C(13) 1.386(9), C(13)-C(19) 1.399(9), C(14)-C(15) 1.388(11), C(14)-C(19) 1.421(10), C(15)-C(16) 1.395(11), C(16)-C(17) 1.375(11), C(17)-C(18) 1.402(10), C(18)-C(19) 1.364(9), C(20)-C(21) 1.412(12), C(21)-C(22) 1.26(2), C(21)-C(22') 1.55(2), C(22)-C(23) 1.34(3), C(23)-C(24) 1.50(3), C(25)-C(24) 1.49(3), C(22')-C(23') 1.37(3), C(23')-C(24') 1.28(3), C(24')-C(25') 1.34(3), C(26)-C(27) 1.445(11), C(27)-C(28) 1.348(11), C(28)-C(29) 1.381(11), C(29)-C(30) 1.435(13), C(30)-C(31) 1.345(12), C(32)-C(33) 1.615(17), C(32)-C(33') 1.66(2), C(34)-C(35) 1.485(11), N(6)-Ni(1)-N(7) 89.5(3), N(6)-Ni(1)-N(5)#1 89.2(3), N(7)-Ni(1)-N(5)#1 92.4(3), N(6)-Ni(1)-N(3) 91.8(4), N(7)-Ni(1)-N(3) 87.4(3), N(5)#1-Ni(1)-N(3) 179.0(3), N(6)-Ni(1)-N(4)#1 100.0(3), N(7)-Ni(1)-N(4)#1 167.6(3), N(5)#1-Ni(1)-N(4)#1 79.9(3), N(3)-Ni(1)-N(4)#1 100.1(3), N(6)-Ni(1)-N(2) 170.8(4), N(7)-Ni(1)-N(2) 90.5(3), N(5)#1-Ni(1)-N(2) 100.1(3), N(3)-Ni(1)-N(2) 79.0(3), N(4)#1-Ni(1)-N(2) 81.4(3)

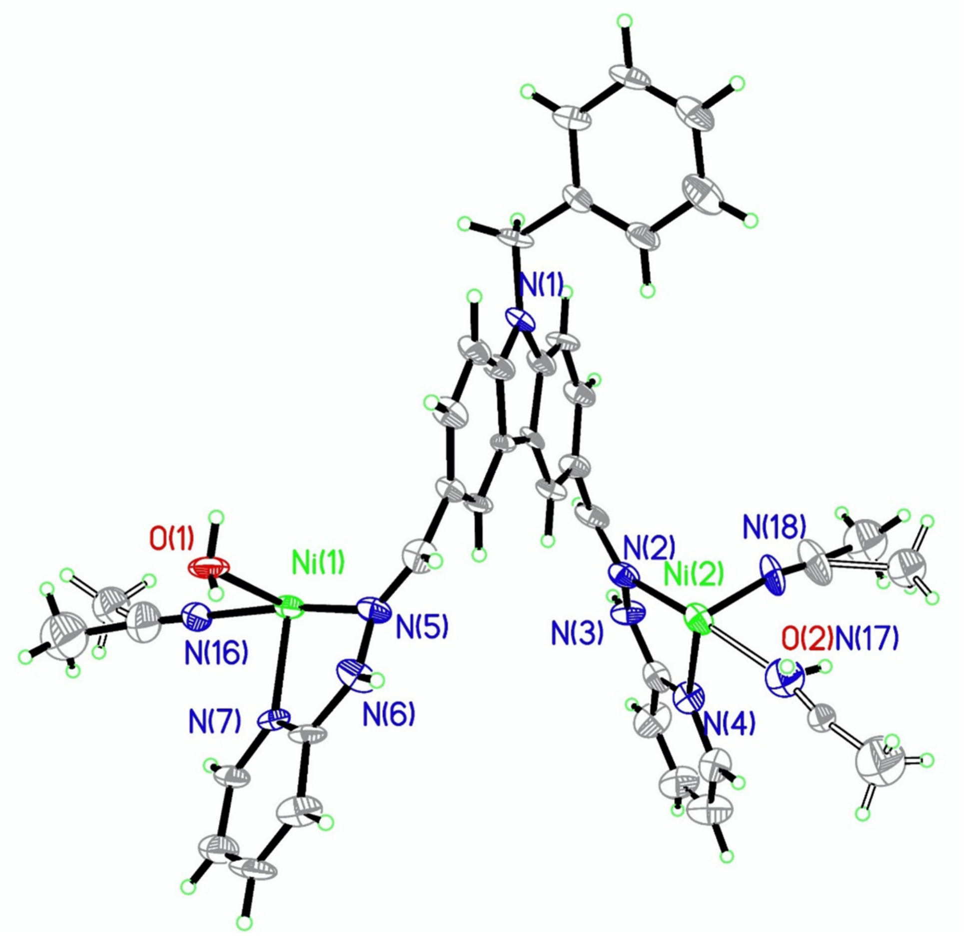

Fig. S3 Molecular structure of Ni-**LA2[44]**, showing the ligand with less extensibility in the complex.

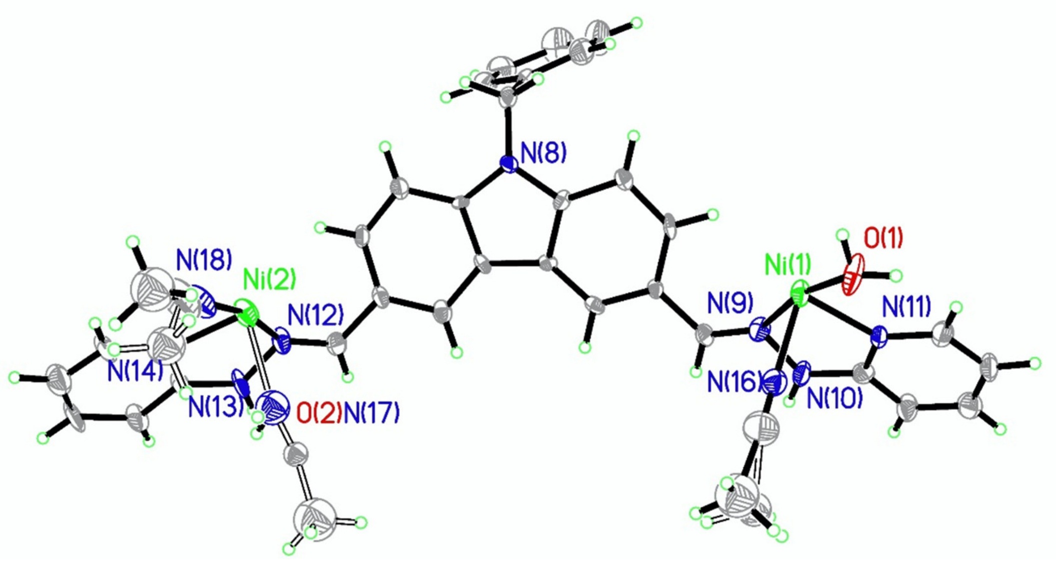

Fig. S4 Molecular structure of Ni-**LA2[44]**, showing the ligand with larger extensibility in the complex.

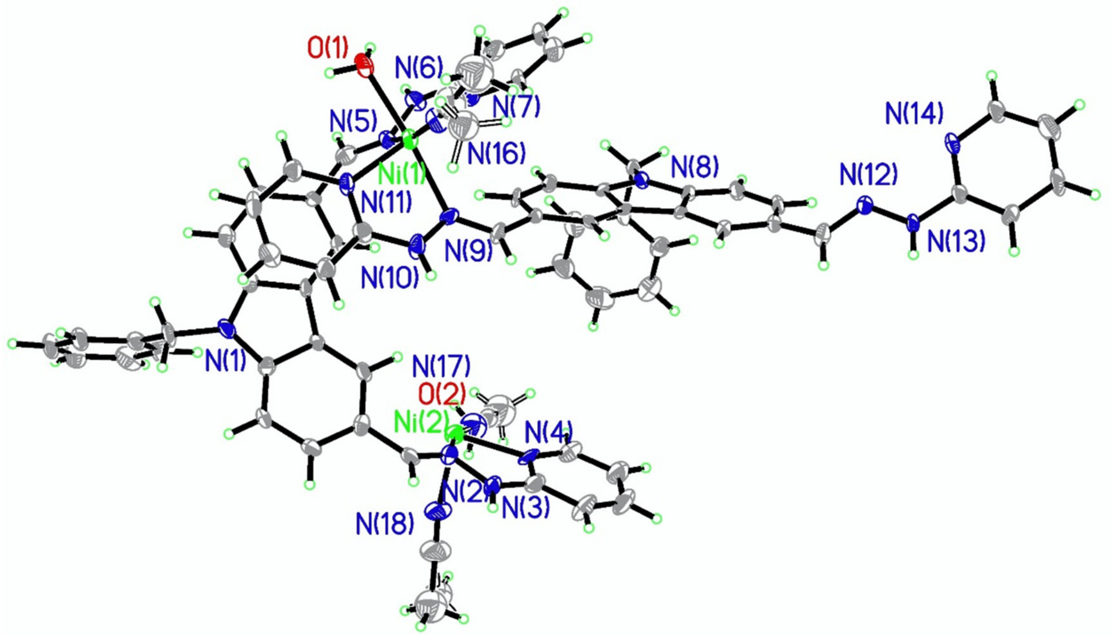

Fig. S5 Coordination geometry of the Ni(1) atom in Ni-**LA2[44].** Selected bond distances (Å) and angles (°): Ni(1)-N(16) 2.032(5), Ni(1)-N(7) 2.039(3), Ni(1)-N(11) 2.042(3), Ni(1)-O(1) 2.104(4), Ni(1)-N(5) 2.115(5), Ni(1)-N(9) 2.141(4), Ni(2)-N(4) 2.022(4), Ni(2)-N(14)#1 2.051(4), Ni(2)-N(18) 2.056(4), Ni(2)-N(2) 2.116(5), Ni(2)-O(2) 2.119(5), Ni(2)-N(12)#1 2.148(4), N(1)-C(7) 1.377(6), N(1)-C(1) 1.379(6), N(1)-C(25) 1.445(6), N(2)-C(13) 1.291(6), N(2)-N(3) 1.374(6), N(3)-C(14) 1.361(6), N(4)-C(14) 1.329(7), N(4)-C(18) 1.373(6), N(5)-C(19) 1.290(6), N(5)-N(6) 1.388(5), N(6)-C(20) 1.372(6), N(7)-C(20) 1.311(7), N(7)-C(24) 1.339(6), N(8)-C(38) 1.376(6), N(8)-C(32) 1.389(5), N(8)-C(56) 1.425(6), N(9)-C(44) 1.266(6), N(9)-N(10) 1.389(5), N(10)-C(45) 1.354(6), N(11)-C(45) 1.317(6), N(11)-C(49) 1.334(6), N(12)-C(50) 1.288(5), N(12)-N(13) 1.387(6), N(12)-Ni(2)#1 2.148(4), N(13)-C(51) 1.359(6), N(14)-C(51) 1.335(6), N(14)-C(55) 1.356(6), N(14)-Ni(2)#1 2.051(4), N(16)-C(65) 1.093(8), N(18)-C(68) 1.098(7), C(1)-C(2) 1.352(7), C(1)-C(6) 1.415(6), C(2)-C(3) 1.373(7), C(3)-C(4) 1.399(6), C(4)-C(5) 1.368(6), C(4)-C(13) 1.436(7), C(5)-C(6) 1.384(7), C(6)-C(12) 1.449(6), C(7)-C(8) 1.379(7), C(7)-C(12) 1.397(6), C(8)-C(9) 1.385(6), C(9)-C(10) 1.370(6), C(10)-C(11) 1.355(7), C(10)-C(19) 1.448(6), C(11)-C(12) 1.397(6), C(14)-C(15) 1.426(8), C(15)-C(16) 1.340(8), C(16)-C(17) 1.383(9), C(17)-C(18) 1.382(8), C(20)-C(21) 1.419(6), C(21)-C(22) 1.364(8), C(22)-C(23) 1.424(9), C(23)-C(24) 1.334(7), C(25)-C(26) 1.515(7), C(26)-C(31) 1.369(8), C(26)-C(27) 1.402(7), C(27)-C(28) 1.362(8), C(28)-C(29) 1.314(8), C(29)-C(30) 1.375(8), C(30)-C(31) 1.405(8), C(32)-C(37) 1.386(7), C(32)-C(33) 1.408(6), C(33)-C(34) 1.404(6), C(34)-C(35) 1.380(7), C(35)-C(36) 1.369(6), C(35)-C(44) 1.453(6), C(36)-C(37) 1.364(6), C(37)-C(43) 1.441(6), C(38)-C(39) 1.376(6), C(38)-C(43) 1.410(6), C(39)-C(40) 1.357(7), C(40)-C(41) 1.390(7), C(41)-C(42) 1.397(6), C(41)-C(50) 1.433(7), C(42)-C(43) 1.401(7), C(45)-C(46) 1.390(6), C(46)-C(47) 1.353(7), C(47)-C(48) 1.370(7), C(48)-C(49) 1.370(6), C(51)-C(52) 1.374(7), C(52)-C(53) 1.413(7), C(53)-C(54) 1.426(8), C(54)-C(55) 1.352(8), C(56)-C(57) 1.506(7), C(57)-C(62)

1.364(7), C(57)-C(58) 1.415(7), C(58)-C(59) 1.367(8), C(59)-C(60) 1.361(9), C(60)-C(61) 1.438(9), C(61)-C(62) 1.336(8), C(65)-C(66) 1.623(11), C(65)-C(66') 1.643(19), C(68)-C(67) 1.486(10), C(68)-C(67') 1.81(5), C(69)-C(70) 1.422(19), N(16)-Ni(1)-N(7) 91.51(17), N(16)-Ni(1)-N(11) 88.90(16), N(7)-Ni(1)-N(11) 178.50(17), N(16)-Ni(1)-O(1) 87.04(18), N(7)-Ni(1)-O(1) 88.70(14), N(11)-Ni(1)-O(1) 92.76(14), N(16)-Ni(1)-N(5) 167.30(15), N(7)-Ni(1)-N(5) 78.89(16), N(11)-Ni(1)-N(5) 100.92(16), O(1)-Ni(1)-N(5) 84.47(17), N(16)-Ni(1)-N(9) 85.02(18), N(7)-Ni(1)-N(9) 99.80(15), N(11)-Ni(1)-N(9) 78.80(15), O(1)-Ni(1)-N(9) 168.50(16), N(5)-Ni(1)-N(9) 104.66(17), N(4)-Ni(2)-N(14)#1 178.25(16), N(4)-Ni(2)-N(18) 87.51(18), N(14)#1-Ni(2)-N(18) 94.05(18), N(4)-Ni(2)-N(2) 78.74(17), N(14)#1-Ni(2)-N(2) 102.17(17), N(18)-Ni(2)-N(2) 85.01(18), N(4)-Ni(2)-O(2) 90.31(19), N(14)#1-Ni(2)-O(2), 88.93(18), N(18)-Ni(2)-O(2) 88.85(19), N(2)-Ni(2)-O(2) 167.64(18), N(4)-Ni(2)-N(12)#1 100.98(15), N(14)#1-Ni(2)-N(12)#1 77.37(15), N(18)-Ni(2)-N(12)#1 168.83(19), N(2)-Ni(2)-N(12)#1 103.64(17), O(2)-Ni(2)-N(12)#1 83.91(17).

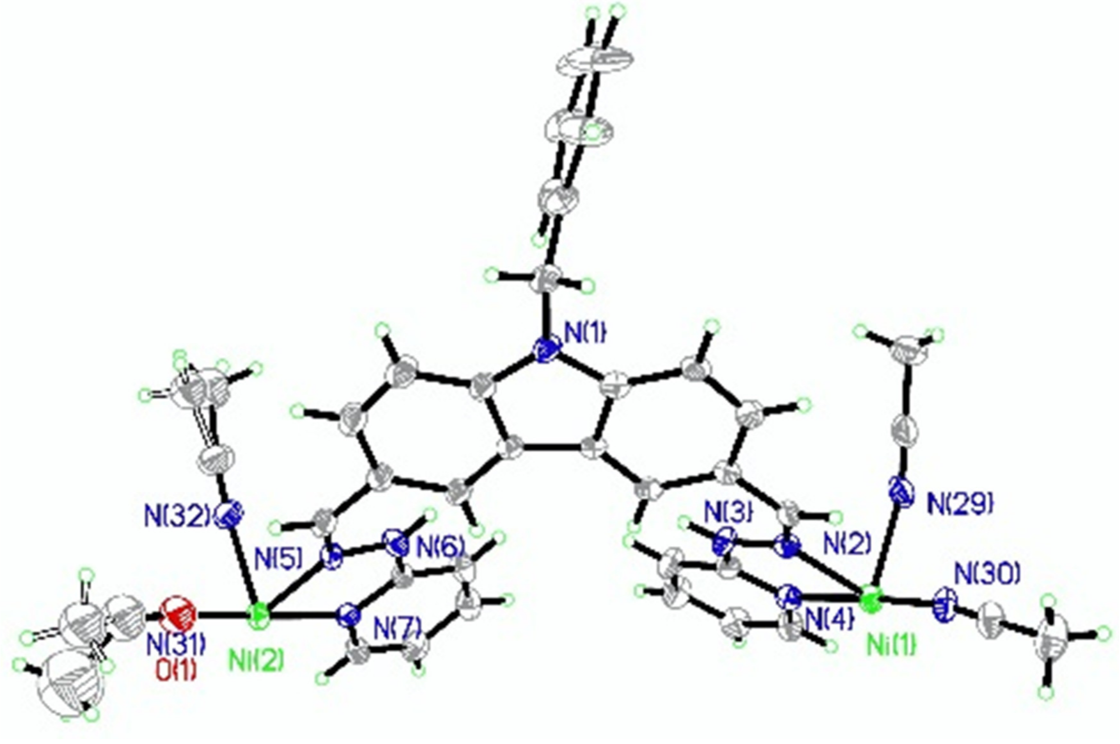

Fig. S6 Molecular structure of Ni-**LA2[22]**, showing the ligand with less extensibility in the complex.

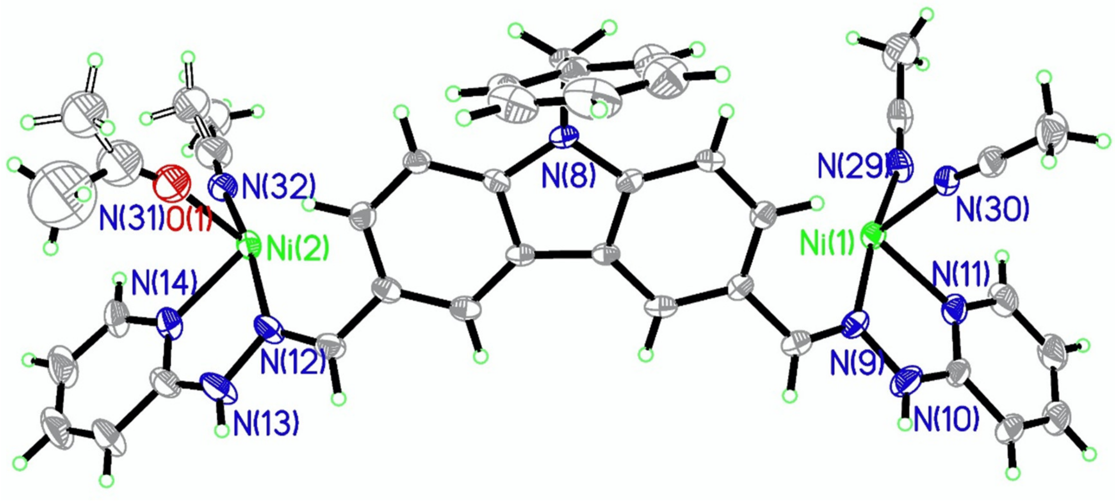

Fig. S7 Molecular structure of Ni-**LA2[22]**, showing the ligand with larger extensibility in the complex.

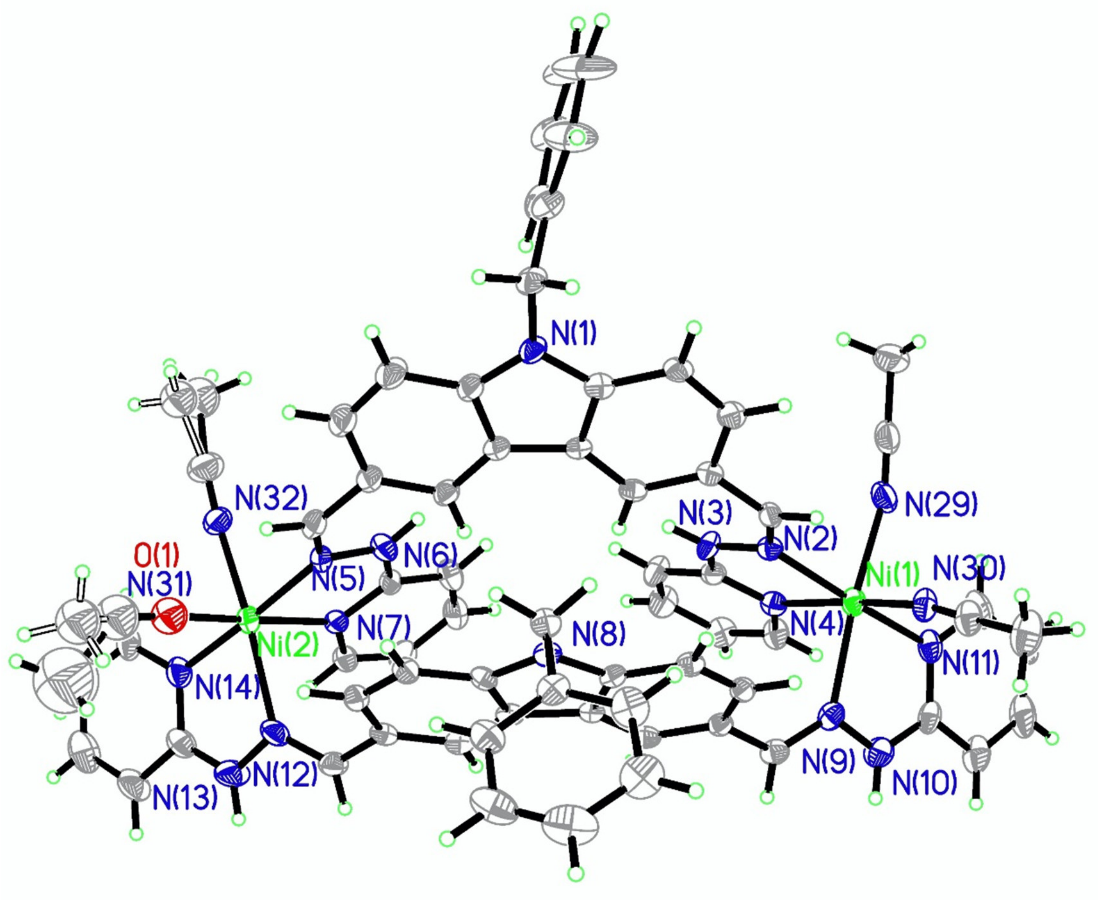

Fig. S8 Coordination geometry of the Ni atom in Ni-**LA2[22].** Selected bond distances (Å) and angles (°): Ni(1)-N(30) 2.044(3), Ni(1)-N(11) 2.048(3), Ni(1)-N(4) 2.053(3), Ni(1)-N(2) 2.083(3), Ni(1)-N(29) 2.091(4), Ni(1)-N(9) 2.156(3), Ni(2)-N(7) 2.048(3), Ni(2)-N(14) 2.063(3), Ni(2)-N(31) 2.069(4), Ni(2)-N(5) 2.069(3), Ni(2)-N(32) 2.106(4), Ni(2)-N(12) 2.180(3), N(1)-C(7)

1.369(5), N(1)-C(1) 1.375(5), N(1)-C(25) 1.452(5), N(2)-C(13) 1.300(5), N(2)-N(3) 1.371(4), N(3)-C(14) 1.384(5), N(4)-C(14) 1.333(5), N(4)-C(18) 1.359(5), N(5)-C(19) 1.308(5), N(5)-N(6) 1.383(4), N(6)-C(20) 1.357(5), N(7)-C(20) 1.339(5), N(7)-C(24) 1.340(5), N(8)-C(32) 1.380(4), N(8)-C(38) 1.393(4), N(8)-C(56) 1.473(4), N(9)-C(44) 1.278(5), N(9)-N(10) 1.376(4), N(10)-C(45) 1.346(5), N(11)-C(45) 1.338(5), N(11)-C(49) 1.365(5), N(12)-C(50) 1.279(5), N(12)-N(13) 1.381(5), N(13)-C(51) 1.334(6), N(14)-C(51) 1.335(6), N(14)-C(55) 1.349(5), N(29)-C(126) 1.117(6), N(30)-C(128) 1.108(5), N(32)-C(132) 1.096(6), C(1)-C(2) 1.397(5), C(1)-C(6) 1.408(5), C(2)-C(3) 1.378(5), C(3)-C(4) 1.395(5), C(4)-C(5) 1.404(5), C(4)-C(13) 1.463(5), C(5)-C(6) 1.387(5), C(6)-C(12) 1.436(5), C(7)-C(8) 1.387(6), C(7)-C(12) 1.403(5), C(8)-C(9) 1.372(6), C(9)-C(10) 1.411(6), C(10)-C(11) 1.386(5), C(10)-C(19) 1.463(6), C(11)-C(12) 1.369(5), C(14)-C(15) 1.380(5), C(15)-C(16) 1.367(6), C(16)-C(17) 1.356(6), C(17)-C(18) 1.353(6), C(20)-C(21) 1.383(5), C(21)-C(22) 1.356(6), C(22)-C(23) 1.392(6), C(23)-C(24) 1.354(6), C(25)-C(26) 1.508(6), C(26)-C(31) 1.379(6), C(26)-C(27) 1.390(6), C(27)-C(28) 1.390(8), C(28)-C(29) 1.409(8), C(29)-C(30) 1.342(8), C(30)-C(31) 1.400(7), C(32)-C(33) 1.399(5), C(32)-C(37) 1.405(5), C(33)-C(34) 1.373(5) , C(34)-C(35) 1.395(5), C(35)-C(36) 1.402(5), C(35)-C(44) 1.463(5), C(36)-C(37) 1.377(5), C(37)-C(43) 1.455(5), C(38)-C(39) 1.384(5), C(38)-C(43) 1.419(5), C(39)-C(40) 1.382(5), C(40)-C(41) 1.418(5), C(41)-C(42) 1.392(5), C(41)-C(50) 1.453(5), C(42)-C(43) 1.383(5), C(45)-C(46) 1.394(6), C(46)-C(47) 1.386(7), C(47)-C(48) 1.396(8), C(48)-C(49) 1.374(7), C(51)-C(52) 1.403(6), C(52)-C(53) 1.374(7), C(53)-C(54) 1.373(8), C(54)-C(55) 1.340(7), C(56)-C(57) 1.501(5), C(57)-C(62) 1.373(6), C(57)-C(58) 1.381(6), C(58)-C(59) 1.420(7), C(59)-C(60) 1.412(7), C(60)-C(61) 1.339(7), C(61)-C(62) 1.413(6), C(127)-C(128) 1.446(6), C(130)-N(31) 1.031(11), C(130)-C(129) 1.468(16), C(130)-C(29') 1.483(15), C(131)-C(132) 1.561(14), C(31')-C(132) 1.440(13), N(30)-Ni(1)-N(11) 90.67(13), N(30)-Ni(1)-N(4) 170.55(13), N(11)-Ni(1)-N(4) 96.43(13), N(30)-Ni(1)-N(2) 94.03(12), N(11)-Ni(1)-N(2) 174.05(13),N(4)-Ni(1)-N(2) 79.30(12), N(30)-Ni(1)-N(29) 91.76(14), N(11)-Ni(1)-N(29) 93.23(14), N(4)-Ni(1)-N(29) 94.04(13), N(2)-Ni(1)-N(29) 83.00(13), N(30)-Ni(1)-N(9) 90.53(13), N(11)-Ni(1)-N(9) 78.45(13), N(4)-Ni(1)-N(9) 84.82(12), N(2)-Ni(1)-N(9) 105.11(12), N(29)-Ni(1)-N(9) 171.39(13), N(7)-Ni(2)-N(14) 98.74(13), N(7)-Ni(2)-N(31) 169.10(13), N(14)-Ni(2)-N(31) 91.13(14), N(7)-Ni(2)-N(5) 79.16(12), N(14)-Ni(2)-N(5) 175.52(14), N(31)-Ni(2)-N(5) 91.30(14), N(7)-Ni(2)-N(32) 91.79(13), N(14)-Ni(2)-N(32) 91.55(14), N(31)-Ni(2)-N(32) 92.56(15), N(5)-Ni(2)-N(32) 84.59(13), N(7)-Ni(2)-N(12) 84.16(12), N(14)-Ni(2)-N(12) 77.85(13), N(31)-Ni(2)-N(12) 93.48(14), N(5)-Ni(2)-N(12) 105.74(12), N(32)-Ni(2)-N(12) 167.88(13).

3. ESI-MS and IM-MS Spectra

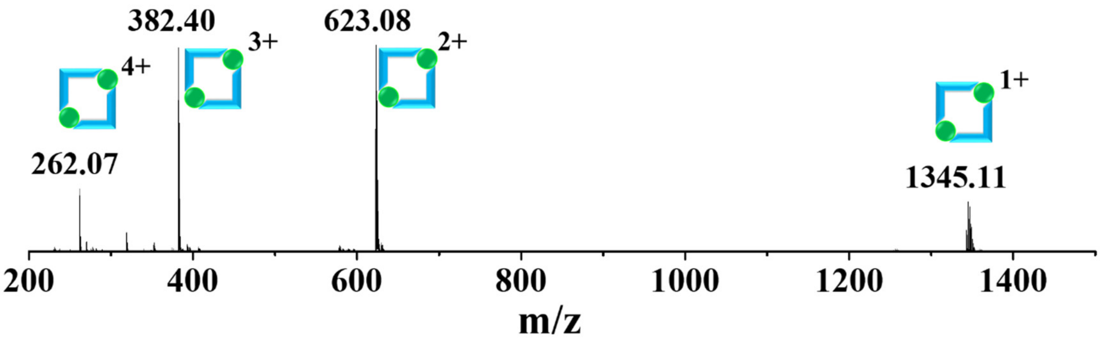

Fig. S9 ESI mass spectrum of Ni-**LA1** in a CH_3CN/CH_3OH (v/v, 9:1) solution.

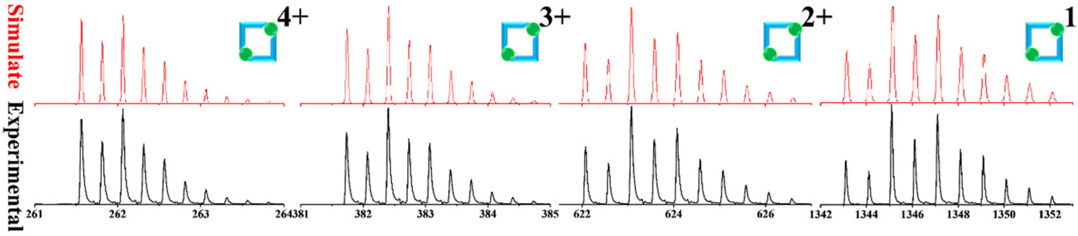

Fig. S10 Ni-**LA1** isotopic distributions for high-resolution mass spectrum peaks.

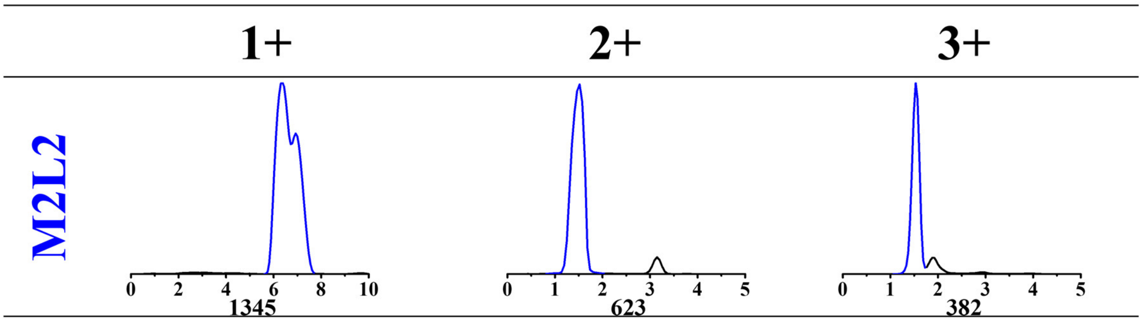

Fig. S11 Drift time distribution for the *m/z* corresponding to the different charge state of Ni-**LA1**.

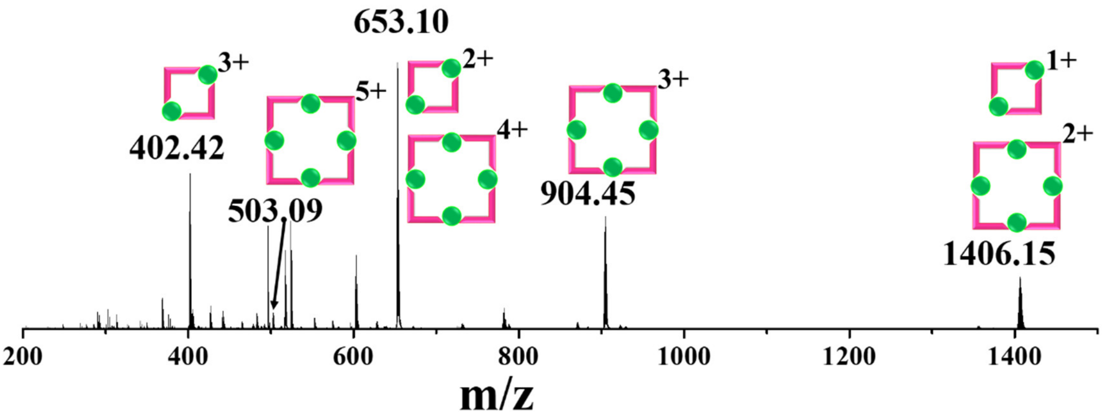

Fig. S12 ESI mass spectrum of Ni-**LA2**.

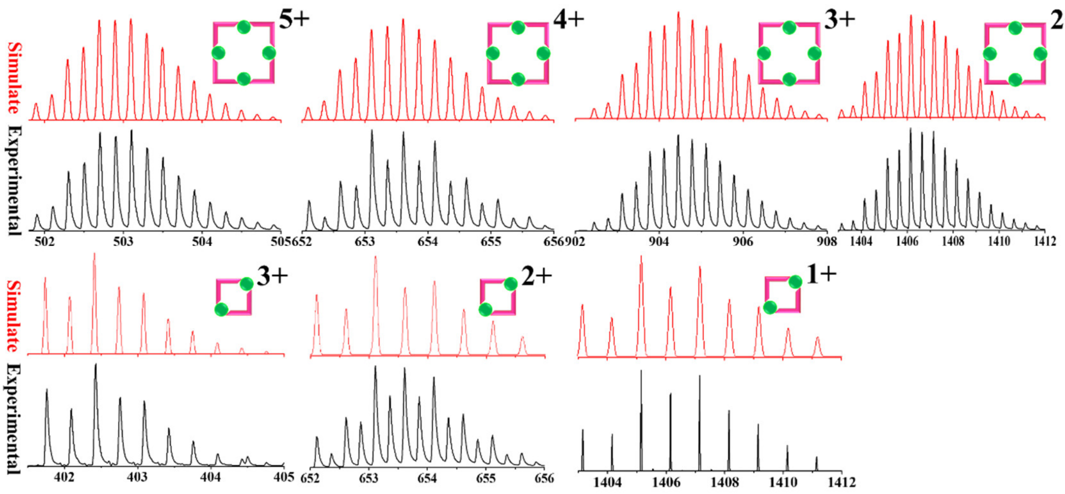

Fig. S13 Ni-**LA2** isotopic distributions for high-resolution mass spectrum peaks.

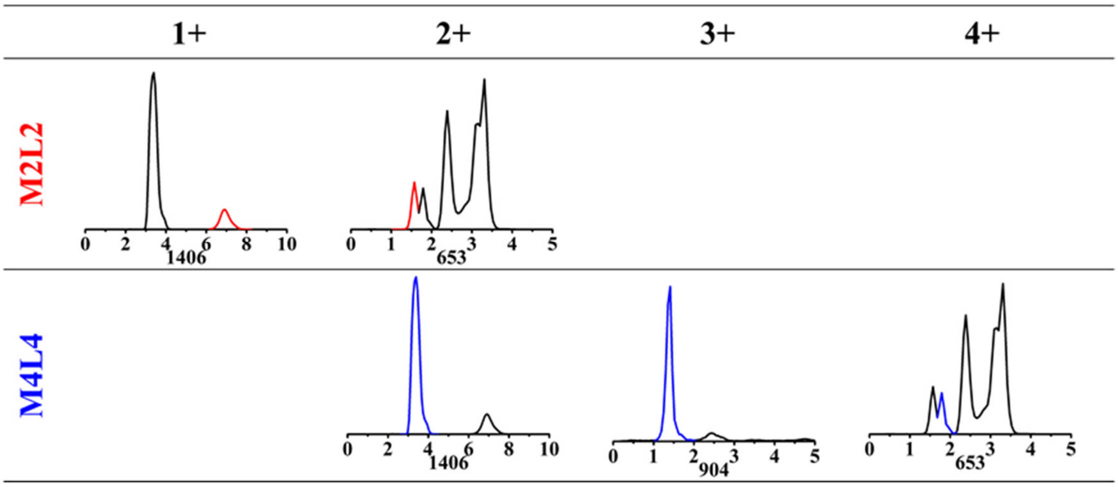

Fig. S14 Drift time distribution for the *m/z* corresponding to the different charge state of Ni-**LA2[44]** and Ni-**LA2[22]** by ion mobility-mass spectrometry.

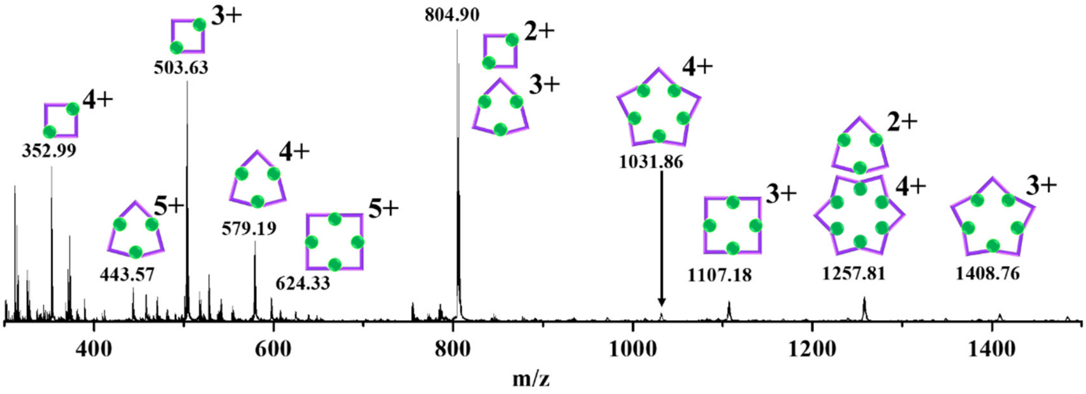

Fig. S15 ESI mass spectrum of Ni-**LA3** in a CH_3CN/CH_3OH (v/v, 9:1) solution.

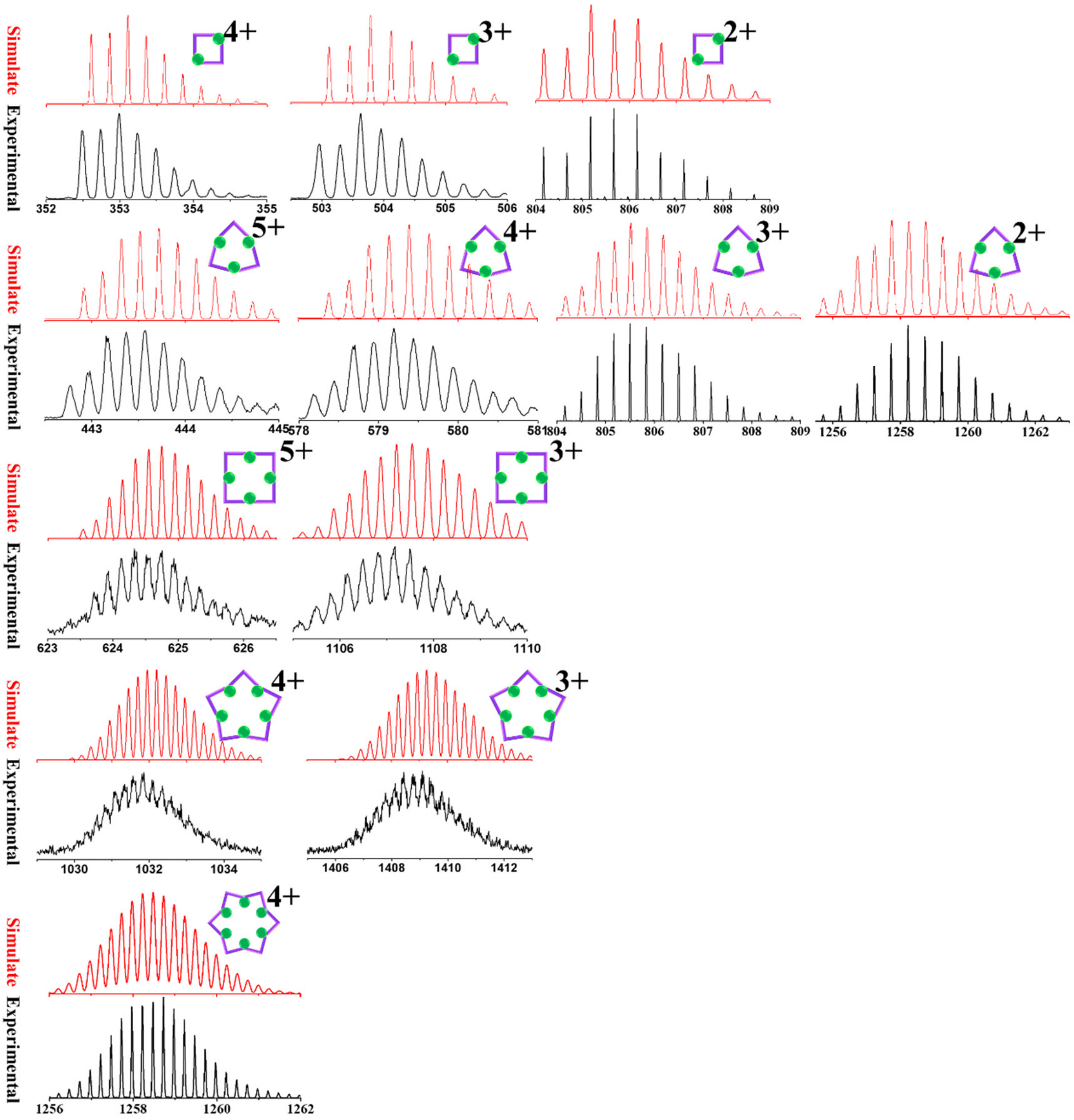

Fig. S16 Ni-**LA3** isotopic distributions for mass spectrum peaks.

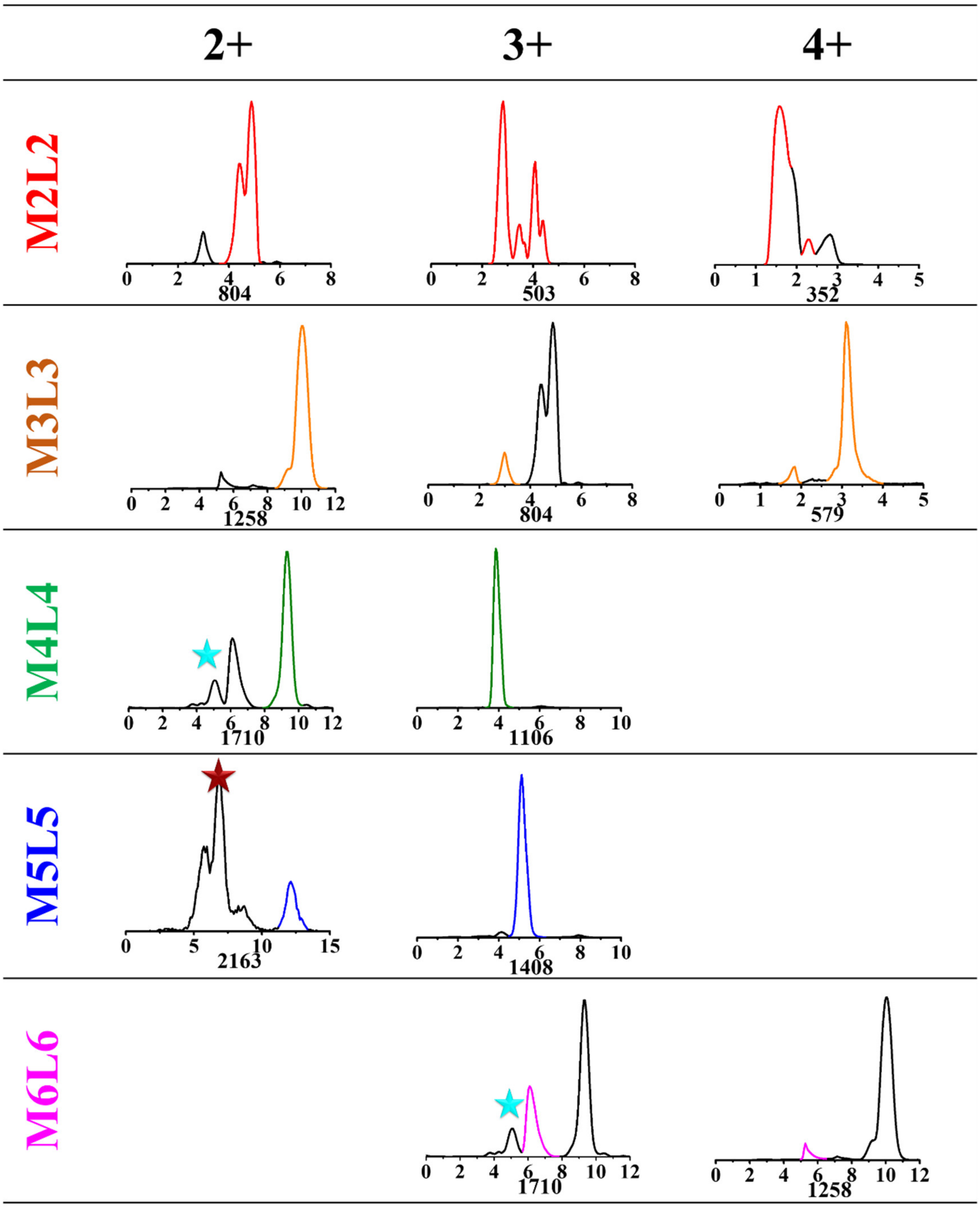

★ The cyan star was a 4-charge peak at m/z = 1710 which was assigned to the specie of $[\mathrm{Ni}_8(\mathbf{LA3})_8(\mathrm{ClO}_4^-)_{12}]^{4+}$.

★ The dark red star was a 4-charge peak at m/z = 2163 which was assigned to the specie of $[\mathrm{Ni}_{10}(\mathbf{LA3})_{10}(\mathrm{ClO}_4^-)_{16}]^{4+}$.

Fig. S17 Drift time distribution for the *m/z* corresponding to different charge state of Ni-**LA3** by ion mobility-mass spectrometry

4. References

[1]. J. T. van Herpt, M. C. A. Stuart, W. R. Browne and B. L. Feringa, *Langmuir*, 2013, 29, 8763-8767.

[2]. G. Li, X. Zhou, P. Yang, Y. Jian, T. Deng, H. Shen and Y. Bao, *Tetrahedron Letters*, 2014, 55, 7054-7059.

[3]. M. Ludwiczak, M. Majchrzak, M. Bayda, B. Marciniak, M. Kubicki and B. Marciniec, *J. Organomet. Chem.*, 2014, 750, 150-161.

[4]. SMART Data collection software, version 5.629; Bruker AXS Inc.: Madison, WI, 2003. SAINT Data reduction software, version 6.45; Bruker AXS Inc.: Madison, WI, 2003.

[5]. G. M. Sheldrick, SHELXTL V5.1, Software Reference Manual, Bruker, AXS, Inc.: Madison, WI, 1997.